RNA (2002), *8*:1068–1077. Cambridge University Press. Printed in the USA.

DOI: 10.1017.S1355838202022033

How Slu7 and Prp18 cooperate in the second step of yeast pre-mRNA splicing

SHELLY-ANN JAMES, WILLIAM TURNER, and BEATE SCHWER

Department of Microbiology and Immunology, Weill Medical College of Cornell University, New York, New York 10021, USA

ABSTRACT

Slu7 and Prp18 act in concert during the second step of yeast pre-mRNA splicing. Here we show that the 382-amino-acid Slu7 protein contains two functionally important domains: a zinc knuckle (^{122}CRNCGEAGHKEKDC^{135}) and a Prp18-interaction domain (^{215}EIELMKLELY^{224}). Alanine cluster mutations of ^{215}EIE^{217} and ^{221}LELY^{224} abrogated Slu7 binding to Prp18 in a two-hybrid assay and in vitro, and elicited temperature-sensitive growth phenotypes in vivo. Yet, the mutations had no impact on Slu7 function in pre-mRNA splicing in vitro. Single alanine mutations of zinc knuckle residues Cys122, His130, and Cys135 had no effect on cell growth, but caused Slu7 function during pre-mRNA splicing in vitro to become dependent on Prp18. Specifically, zinc knuckle mutants required Prp18 in order to bind to the spliceosome. Compound mutations in both Slu7 domains (e.g., C122A-EIE, H130A-EIE, and C135A-EIE) were lethal in vivo and abolished splicing in vitro, suggesting that the physical interaction between Slu7 and Prp18 is important for cooperation in splicing. Depletion/reconstitution studies coupled with immunoprecipitations suggest that second step factors are recruited to the spliceosome in the following order: Slu7 → Prp18 → Prp22. All three proteins are released from the spliceosome after step 2 concomitant with release of mature mRNA.

Keywords: Prp22; Prp43; spliceosome; zinc knuckle

INTRODUCTION

Introns are removed from pre-mRNAs via two sequential transesterification steps. In the first step, the 5′ splice site is cleaved and the branched lariat-exon 2 and exon 1 intermediates are formed. In the second step, the 3′ splice site is cleaved and the exons are joined (Moore et al., 1993). Pre-mRNA splicing is catalyzed by the spliceosome, a large complex composed of snRNPs and non-snRNP proteins that associate with the precursor RNA (Staley & Guthrie, 1998; Burge et al., 1999; Stevens et al., 2002). Numerous RNA–RNA and RNA–protein interactions are involved in the recognition and selection of the splice sites (Madhani & Guthrie, 1994; Nilsen, 1994). In yeast, spliceosome assembly and the first transesterification step can occur in the absence of a 3′ splice site PyAG↓ (↓ indicates the cleavage site), implying that the site is recognized after step 1 (Rymond & Rosbash, 1985; Vijayraghavan et al., 1986). Positioning of the active site for step 2 transesterification involves the U5 snRNA, the Prp8 protein, and other factors that function specifically during step 2 (Umen & Guthrie, 1995a, 1995b; Newman, 1997). The latter include Prp16, Slu7, Prp18, and Prp22 (Schwer & Guthrie, 1991; Horowitz & Abelson, 1993a; Schwer & Gross, 1998).

ATP hydrolysis by Prp16 effects a conformational rearrangement in the spliceosome that can be measured as protection of the 3′ splice site region from oligo-directed RNase H cleavage, presumably because it is bound by proteins or snRNPs (Schwer & Guthrie, 1992). Slu7, Prp18, and Prp22 are recruited during this stage of step 2, and they promote step 2 catalysis independent of ATP (Horowitz & Abelson, 1993a, 1993b; Ansari & Schwer, 1995; Jones et al., 1995; Schwer & Gross, 1998).

The essential *SLU7* gene was identified in a screen for mutants that exacerbate the temperature-sensitive phenotype of a U5 snRNA mutation (Frank et al., 1992; Frank & Guthrie, 1992). *SLU7* encodes a 382-amino-acid protein, which contains in its N-terminal segment a zinc knuckle motif (^{122}CRNCGEAGHKEKDC). Although the zinc knuckle is conserved in Slu7 orthologs from other fungi and metazoa, mutational studies showed that it is not essential for cell growth (Frank & Guthrie, 1992; Zhang & Schwer, 1997; Chua & Reed, 1999; Käufer & Potashkin, 2000).

Reprint requests to: Beate Schwer, Department of Microbiology and Immunology, Weill Medical College of Cornell University, New York, New York 10021, USA; e-mail: bschwer@mail.med.cornell.edu.

Slu7 interacts with Prp18 in a two-hybrid assay and the segment of Slu7 from amino acids 200 to 224 is necessary for this interaction (Zhang & Schwer, 1997). *PRP18* is not essential for cell growth; however *prp18*Δ cells grow slowly at temperatures below 30 °C and they do not grow at >30 °C (Horowitz & Abelson, 1993a). In vitro splicing in extracts depleted of Prp18 and Slu7 can be restored by purified Prp18 and Slu7 proteins (Horowitz & Abelson, 1993b; Ansari & Schwer, 1995). The requirement for Prp18 can be bypassed by the addition of high concentration of Slu7, but not vice versa (Zhang & Schwer, 1997). These studies showed that Prp18 and Slu7 cooperate to promote the second step of splicing. A model in which Prp18 facilitates Slu7 function is supported by numerous genetic data, including dosage suppression and synergistic lethality, which establish a network of interaction between the U5 snRNP and second step factors, including Slu7 and Prp18 (Frank & Guthrie, 1992; Jones et al., 1995; Ben-Jehuda et al., 2000).

Here, we sought to determine whether the physical interaction between Slu7 and Prp18 is a prerequisite for their cooperation in pre-mRNA splicing and to explore the molecular basis thereof. We show that Slu7 contains two important regions, the zinc knuckle motif and the Prp18-interaction region. Either one of the two domains is necessary for Slu7 function. Slu7 mutants in which conserved cysteines or a histidine residue in the zinc knuckle were individually replaced by alanine are dependent on interaction with Prp18 for spliceosome binding, for in vitro splicing activity, and for cell growth. Using immunoprecipitation assays, we establish that Slu7 is required for the recruitment of Prp18 and Prp22 to the spliceosome and that Slu7, Prp18, and Prp22 dissociate from the splicing complex concomitant with the release of mRNA and prior to the release of lariat-intron from the remaining complex.

RESULTS

Splicing activity of Slu7 deletion mutants

Previous studies showed that deletion of up to 80 amino acids from the N-terminus of Slu7 had no effect on cell growth (Zhang & Schwer, 1997). N-terminal deletions of 124, 162, 183, and 199 amino acids caused temperature-sensitive phenotypes in vivo, whereas deleting 221 amino acids was lethal. Here we purified the truncated Slu7 proteins Δ80, Δ124, Δ162, Δ183, Δ199, and Δ221, and tested their splicing activities in vitro in a yeast extract depleted of both Slu7 and Prp18 (Fig. 1). The purities of the protein preparations were comparable (Fig. 1A). His_{10}-Slu7 migrated at 55 kDa, which is slightly larger than the calculated molecular mass of 48 kDa. The truncated His_{10}-Slu7 mutant polypeptides migrated incrementally faster, consistent with the extent of their N-terminal deletions.

When ^{32}P-labeled actin pre-mRNA was incubated in Δ7Δ18 extract, the first step of splicing occurred and lariat-exon 2 and exon 1 accumulated (Fig. 1B,C, lane −). Mature mRNA was formed upon addition of purified recombinant wild-type Slu7 and Prp18 (30 ng each; Fig. 1C, lane Slu7). Whereas wild-type Slu7 did promote mRNA formation in the absence of added Prp18, the truncated Slu7 proteins did not (Fig. 1B). Yet, the Δ80, Δ124, Δ162, Δ183, and Δ199 mutants were all active in the presence of Prp18 (Fig. 1C). The Δ221 mutant, which was lethal in vivo, did not promote mRNA formation with or without Prp18. At much larger amounts of input Slu7 (400 ng), the Δ80 mutant was

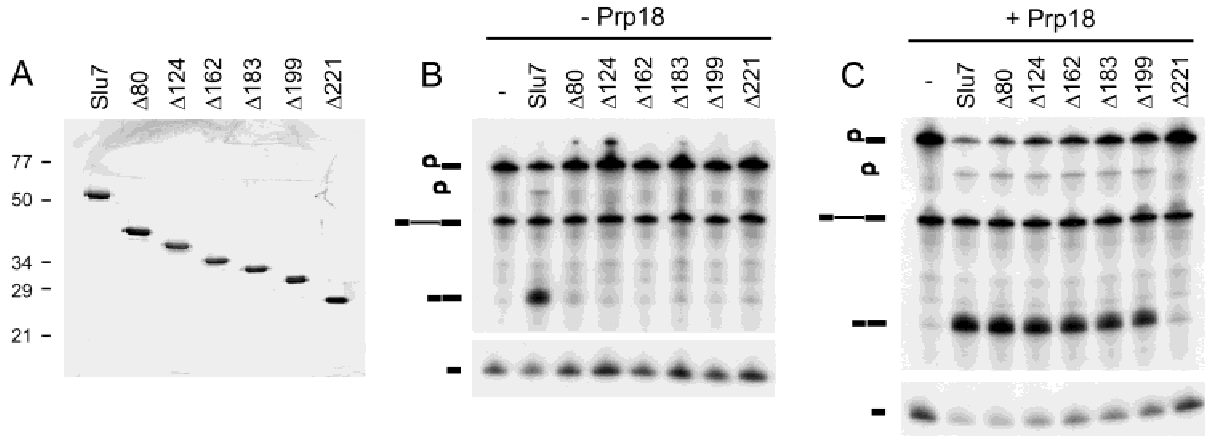

FIGURE 1. Slu7 truncation mutants. **A:** Slu7 proteins (1 μg each) were separated by 12% SDS-PAGE and visualized with Coomassie staining. The positions and sizes (in kilodaltons) of marker proteins are indicated at the left. **B, C:** In vitro splicing activities of truncated Slu7 mutants. ^{32}P-labeled actin pre-mRNA was reacted with Δ7Δ18 extract for 15 min at 23 °C to allow for step 1 to occur. Aliquots of the reaction mixtures were then supplemented with 30 ng of the Slu7 proteins as indicated in the absence (**B**) or presence (**C**) of Prp18 (30 ng). After incubation for 15 min at 23 °C, the RNA products were analyzed by denaturing PAGE and visualized by autoradiography. The symbols at the left indicate the corresponding RNA species. These are from top to bottom: lariat-exon 2, lariat-intron, precursor, mRNA, and exon 1.

active in the absence of Prp18, but the Δ124, Δ162, Δ183, and Δ199 proteins were not (data not shown). We infer from the results that loss of the N-terminal domain of Slu7 renders it Prp18-dependent for splicing in vitro.

Effect of zinc knuckle mutations on Slu7 function in vitro

Slu7 contains a zinc knuckle motif ^{122}CRNCGEAGH KEKDC^{135} (Fig. 2) that is conserved in other Slu7 orthologs, yet dispensable for yeast cell growth at temperatures below 37 °C (Frank & Guthrie, 1992; Zhang & Schwer, 1997). It is conceivable that Slu7 deletion mutants Δ124 to Δ199 were dependent on Prp18 because they lacked a zinc knuckle motif. To test this, we individually substituted the defining residues Cys122, His130, and Cys135 by Ala, purified the Slu7-Ala proteins from *Escherichia coli*, and assayed them for pre-mRNA splicing in vitro in the Δ7Δ18 extract. The splicing activities of the C122A, H130A, and C135A mutants were dependent on Prp18 (Fig. 4, lanes 5 and 11; data not shown). We infer that the zinc knuckle plays a role in the ability of Slu7 to bypass the requirement for Prp18 in vitro.

Mapping the Prp18-interaction site in Slu7

A segment in Slu7 that spans amino acids 200 to 224 is necessary for its interaction with Prp18 in a two-hybrid assay (Zhang & Schwer, 1997). To determine which residues are important for the interaction, we replaced clusters of three or four neighboring amino acids by alanine and tested their abilities to interact with Prp18. The Slu7-Ala mutants ^{203}SQT, ^{206}DET, ^{209}LWD, ^{212}TDE, ^{215}EIE, ^{218}LMK, and ^{221}LELY were fused to the Gal4 DNA-binding domain (GBD). Plasmids carrying *GBD-SLU7-Ala* mutants were introduced into strain Y187 together with a plasmid expressing Prp18 fused to the Gal4 activation domain (pGAD-PRP18). Leu$^+$Trp$^+$ transformants were tested for expression of the *lacZ* reporter gene. The results are summarized in Figure 2. Replacing ^{203}SQT, ^{206}DET, ^{209}LWD, ^{212}TDE, and ^{218}LMK by AAA did not affect the interaction of the fusion protein with Prp18, that is, the cells were blue in X-Gal. However, replacing ^{215}EIE by AAA or ^{221}LELY by AAAA abolished the interaction with Prp18 and the cells were white. When residues within the ^{215}EIE and ^{221}LELY peptides were individually replaced by alanine, we found that E217A abolished the ability of the fusion protein to interact with Prp18, but none of the other single alanine substitution mutants (E215A, I216A, L221A, E222A, L223A, and Y224A) affected *lacZ* expression (Fig. 2; data not shown).

Prp18-Slu7 interaction in vitro

Purified recombinant His$_6$-Prp18 was mixed with untagged, partially purified wild-type Slu7 or with the Slu7-Ala mutants ^{215}EIE, ^{221}LELY, E215A, and E217A (Fig. 3). The mixtures were then adsorbed to Ni-agarose resin. The Ni-resin was collected by centrifugation and the supernatant removed. The pellet was washed, the bound proteins were eluted with 0.5 M imidazole, and the bound

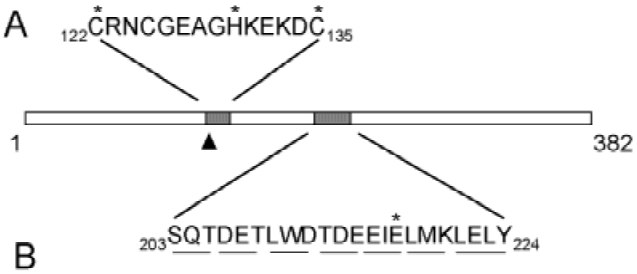

	growth (5-FOA)	15°	30°	37°	2-hybrid Prp18
Slu7	+	+++	+++	+++	+
Δ124	+	+++	+++	-	+
C122A	+	+++	+++	+++	*nd*
H130A	+	+++	+++	+++	*nd*
C135A	+	+++	+++	+++	*nd*
SQT	+	+++	+++	+++	+
DET	+	+++	+++	+++	+
LWD	+	+++	+++	+++	+
TDE	+	+++	+++	+++	+
EIE	+	+++	+++	-	-
LMK	+	+++	+++	+++	+
LELY	+	+++	+++	+	-
E215A	+	+++	+++	+++	+
I216A	+	+++	+++	+++	+
E217A	+	+++	+++	+++	-
Δ124-EIE	-				
Δ124-E217A	-				
C122A-EIE	-				
C122A-E217A	+	++	+	-	
H130A-EIE	-				*nd*
H130A-E217A	+	++	++	-	
C135A-EIE	-				
C135A-E217A	+	+++	+	-	

FIGURE 2. Mutational analysis of Slu7. **A:** Slu7 is drawn as a horizontal bar, with the shaded segments indicating the zinc knuckle motif and the Prp18-interaction region. The amino acid sequences of the zinc knuckle and the Prp18-binding region are shown in the expanded view above and below the horizontal bar, respectively. The numbers refer to the amino acids in Slu7. The lines below the sequence of the Prp18-binding region highlight positions that were replaced by alanine in clusters of three and four. The stars highlight positions that are important for Slu7 function. **B:** Summary of mutational effects. The ability of the various *slu7* alleles to complement a *slu7*Δ strain was tested by plasmid shuffle. + indicates that the mutant allele supported the formation of colonies on 5-FOA containing medium and − indicates lethality on 5-FOA at 25 °C and 30 °C. Viable mutants were streaked to rich medium (YPD) and incubated at 15 °C, 30 °C, and 37 °C. Growth was scored based on colony size after incubation for 9 days at 15 °C or 3 days at 30 dgC and 37 °C. +++: growth comparable to wild-type *SLU7*; ++: slow growth; + only pinpoint colonies formed; −: no colonies formed. The two-hybrid interaction of the various GBD-Slu7 mutants with Prp18 (fused to the Gal4 activation domain) was assessed using the *lacZ* reporter assay. +: interaction, that is, blue color on X-gal; −: no interaction; *nd*: not determined.

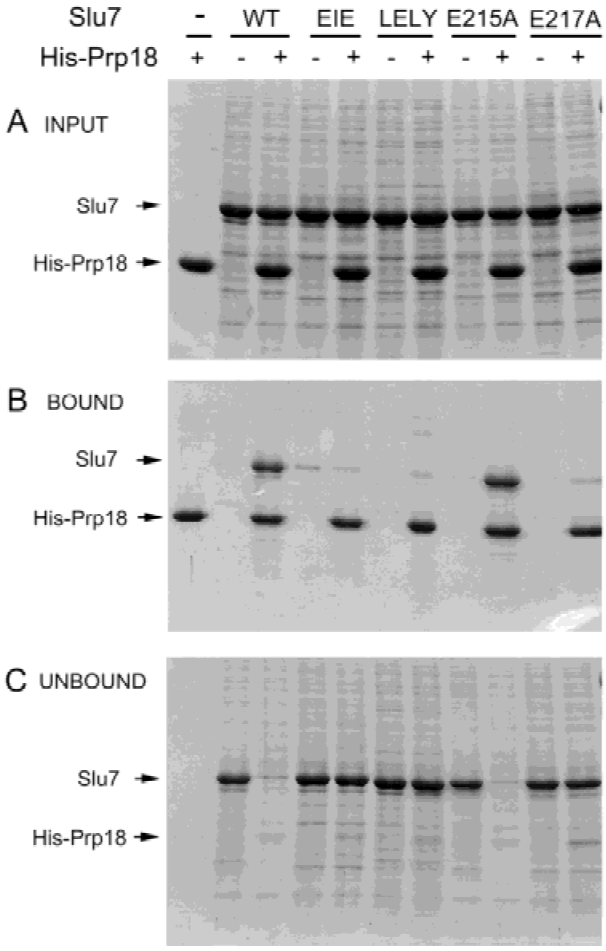

FIGURE 3. Slu7-Prp18 interaction in vitro. Purified His-Prp18 and partially purified Slu7 proteins were mixed as indicated. Aliquots of (**A**) the input mixtures (10 μL of 400 μL were loaded), (**B**) the proteins eluted from the Ni-agarose resin (5 μL of 150 μL), and (**C**) the supernatants after binding to the beads (10-μL aliquots) were analyzed by 10% SDS-PAGE. Polypeptides were stained with Coomassie blue. The positions of Slu7 and His-Prp18 proteins are indicated at the left.

and free fractions were analyzed by SDS-PAGE (Fig. 3B). Prp18 bound to the Ni-resin by virtue of its His_6-tag. The Slu7 proteins did not bind to the resin in the absence of His_6-Prp18. However, when mixed with His-Prp18, wild-type Slu7 and E215A were recovered in the bound fractions (Fig. 3B) and the majority of Slu7 and E215A was depleted from the supernatant (Fig. 3C). In contrast, ^{215}EIE, ^{221}LELY, and E217A were not recovered in the bound fraction, indicating that these proteins failed to interact with Prp18. This result confirms our findings from the two-hybrid assay and argues that the Slu7 and Prp18 proteins interact directly.

The in vivo function of Slu7-Ala mutants

If the physical interaction with Prp18 is important for Slu7 function, we would expect that Slu7 mutations that disrupt Prp18 binding might elicit growth phenotypes. The most severe defect would resemble the phenotype of a *prp18*Δ strain, which grows slowly at 25 °C, forms pinpoint colonies at 30 °C, and does not form colonies at ≥32 °C (Horowitz & Abelson, 1993a). The *SLU7-Ala* alleles *SQT*, *DET*, *LWD*, *TDE*, *EIE*, *LMK*, and *LELY* on *CEN TRP1* plasmids were introduced into a *slu7*Δ strain carrying a *URA3 SLU7 CEN* plasmid. Trp$^+$ transformants were plated on medium containing 5-fluoroorotic acid (5-FOA), a drug that selects against the *URA3 SLU7* plasmid. All of the alanine-cluster substitution mutants formed colonies on 5-FOA at 25 °C and 30 °C (Fig. 2). The individual Slu7-Ala strains were then tested for growth on rich medium (YPD) at 15 °C, 30 °C, and 37 °C. We found that replacing ^{215}EIE by ^{215}AAA or ^{221}LELY by ^{221}AAAA caused a temperature-sensitive growth defect, whereby *EIE* did not form colonies at 37 °C and *LELY* formed only pinpoint colonies (Fig. 2B). When Glu215, Ile216, and Glu217 in ^{215}EIE and Leu221, Glu222, Leu223, and Tyr224 in ^{221}LELY were replaced individually by alanine, none of the single substitution mutations exerted a growth phenotype (Fig. 2B; data not shown).

The E217A mutation disrupted the ability of Slu7 to interact with Prp18, yet *E217A* cells did not display an overt growth phenotype. To better understand the contributions of Glu217 to Prp18 binding, we introduced conservative mutations (to Gln and Asp) and inverted the charge (to Lys). E217Q and E217D interacted with Prp18 in the two-hybrid assay, whereas E217K did not (data not shown). *E217Q* and *E217D* cells had no growth phenotype, whereas *E217K* was temperature sensitive (data not shown). We conclude that the physical interaction between full-length Slu7 and Prp18 is not strictly essential for growth, but that the interaction is beneficial at 37 °C. The growth defects of the mutants *EIE*, *LELY*, and *E217K* were not ameliorated by overexpression of the Slu7-ts mutants (data not shown).

The physical interaction between Slu7 and Prp18 is a prerequisite for cooperation in splicing

Mutations C122A, H130A, C135A, and Δ124 render the in vitro splicing activity of Slu7 dependent on Prp18 (Fig. 1B,C; Fig. 4; data not shown). The EIE and E217A mutants, which fail to interact with Prp18, promoted mRNA formation in the absence and presence of Prp18 (Fig. 4). We combined the individual mutations to generate Slu7 compound mutants C122A-E217A, C122A-EIE, H130A-E217A, H130A-EIE, C135A-E217A, C135A-EIE, Δ124-E217A, and Δ124-EIE. We then tested their function in vivo and in vitro.

We found that C122A-EIE, H130A-EIE, C135A-EIE, Δ124-EIE, and Δ124-E217A did not support growth of a *slu7*Δ strain, whereas the C122A-E217A, H130A-E217A, and C135A-E217A cells grew slowly at 15 °C,

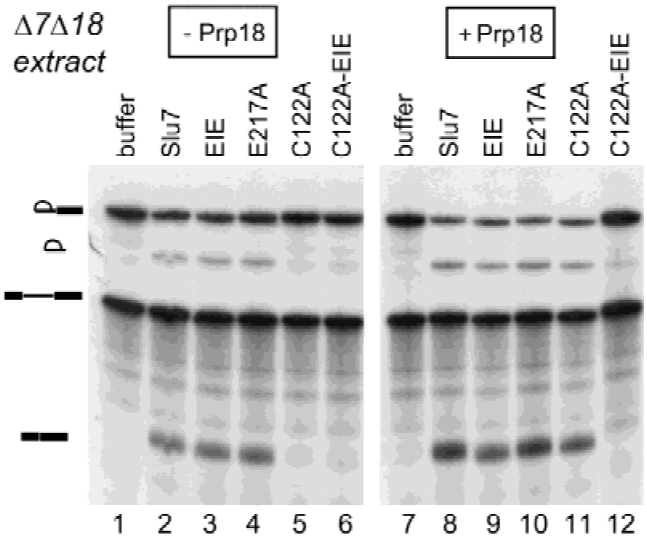

FIGURE 4. In vitro splicing. ^{32}P-labeled actin pre-mRNA was reacted with extract depleted of Slu7 and Prp18 (Δ7Δ18) for 15 min at 23 °C. Aliquots of the mixture were then supplemented with 30 ng of the indicated proteins. After an additional 15 min at 23 °C, splicing was halted, and the RNA was extracted and analyzed by denaturing PAGE and autoradiography. The symbols at the left identify the RNA. These are from top to bottom: lariat-exon 2, lariat-intron, precursor, mRNA. Exon 1 migrates ahead of mRNA and is not shown.

formed pinpoint colonies at 30 °C, and failed to grow at 37 °C (Fig. 2B). Thus, mutations in the zinc knuckle exacerbated the phenotypes elicited by mutations in the Prp18-interaction region and vice versa. This suggested functional redundancy between the two regions in Slu7.

We purified the C122A-EIE, H130A-EIE, and C135A-EIE mutants and tested their splicing activities in vitro. C122A-EIE failed to promote mRNA formation, whether Prp18 was added or not (Fig. 4, lanes 6 and 12). Similarly, H130A-EIE and C135A-EIE were inactive in the absence or presence of Prp18 (data not shown). These results indicated that the physical interaction between Slu7 and Prp18 is important for their functional cooperation in splicing.

Spliceosome association of the mutant Slu7 proteins

Using Δ7Δ18 extract and purified proteins, we assessed the association of Slu7 mutants with splicing complexes. To prevent conversion of intermediates to spliced mRNA when both proteins are added, we employed a mutant actin precursor RNA (C303/305) containing a mutation at the 3′ splice site. The splice site mutation prevents step 2 transesterification, but it does not interfere with the Prp16-catalyzed conformational change that leads to the protection of the 3′ splice site and requires recruitment of Slu7, Prp18, and Prp22 (Vijayraghavan et al., 1986; Schwer & Guthrie, 1992; Schwer & Gross, 1998). The ^{32}P-labeled C303/305 precursor RNA was incubated with Δ7Δ18 extract and aliquots of the reaction mixture were then supplemented with purified Slu7 and Prp18 and subjected to immunoprecipitation with anti-Slu7 antibodies (Fig. 5). Wild-type Slu7 bound to spliceosomes after step 1, insofar as Slu7-specific antibodies coprecipitated ^{32}P-labeled lariat-exon 2 and exon 1, but not unspliced pre-mRNA (Fig. 5). Slu7 bound to spliceosomes whether Prp18 was added or not (Fig. 5, lanes 9 and 12). In contrast, the Slu7-C135A mutant bound to the spliceosome only when Prp18 was added (Fig. 5, lanes 10 and 13). The compound mutant C135A-EIE did not bind to spliceosomes even when Prp18 was added (Fig. 5, lanes 11 and 14). The C122A and H130A mutants depended on Prp18 for spliceosome binding, and the compound mutants C122A-EIE and H130A-EIE failed to bind to spliceosomes even in the presence of Prp18 (data not shown). These findings establish a correlation between the ability of Slu7 to function in pre-mRNA splicing and its ability to bind stably to spliceosomes. We surmise that functional cooperation between Slu7 and Prp18 occurs at the level of spliceosome binding and that the direct physical interaction of Slu7 with Prp18 is important at this stage.

Ordered binding of second step factors to the spliceosome

Slu7, Prp18, and Prp22 function during the ATP-independent stage of step 2 after Prp16. Do Slu7, Prp18, and Prp22 associate with the spliceosome indepen-

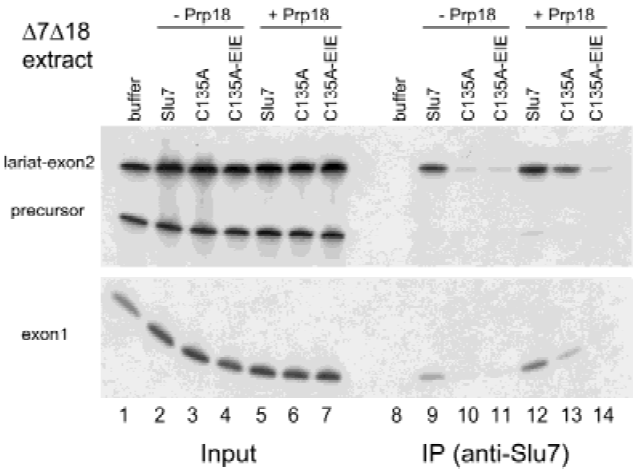

FIGURE 5. Spliceosome binding. ^{32}P-labeled C303/305 precursor RNA was incubated in Δ7Δ18 extract to generate lariat-exon 2 and exon 1 intermediates. Aliquots (40 μL) of the reaction mixture were supplemented with Slu7 proteins as indicated either in the absence or presence of Prp18. One-quarter of the reaction mixture served as input and three-quarters were subjected to immunoprecipitation with anti-Slu7 antibodies. RNAs in the input and precipitated samples were analyzed by denaturing PAGE and autoradiography.

dently of each other or is there an order for binding? We used depletion/reconstitution assays and immunoprecipitation to address this question. Spliceosomes containing the products of step 1 were formed on C303/305 precursor RNA in Δ7Δ18 or Δ22 extracts. Aliquots of the reaction were then supplemented with recombinant proteins and subjected to immunoprecipitation with anti-Prp18, anti-Slu7, and anti-Prp22 antibodies (Fig. 6). Anti-Prp18 antibodies precipitated splicing intermediates from reaction mixtures that were supplemented with Slu7 plus Prp18, but not with Prp18 alone, showing that Prp18 requires Slu7 for binding to splicing complexes (Fig. 6A, lanes 5 and 6). In contrast, Slu7 associated with spliceosomes even in the absence of Prp18 (Figs. 5 and 6A). Increasing the salt concentration during immunoprecipitation from 150 to 200 mM reduced the efficiency of spliceosome precipitation by anti-Slu7 antibodies disproportionately when Prp18 was absent, indicating that Prp18 may stabilize the binding of Slu7 (data not shown).

Splicing intermediates formed in Δ7Δ18 extract (containing endogenous Prp22) were precipitated efficiently with anti-Prp22 antibodies only when both Slu7 plus Prp18 were added; no intermediates were precipitated in the absence of Slu7 and only small amounts were precipitated when Prp18 was omitted (Fig. 6A, lanes 17–20). The finding that Prp22 can associate with spliceosomes in the absence of Prp18 (albeit at greatly reduced efficiency) is consistent with the finding that Prp18 is not essential for pre-mRNA splicing in vitro.

Slu7 and Prp18 antibodies precipitated splicing intermediates that were formed in extracts lacking Prp22 (Fig. 6B). Thus, whereas Slu7 and Prp18 bound independent of Prp22, the association of Prp22 with splicing complexes required Slu7 and Prp18. These result imply an order for spliceosome binding: Slu7 → Prp18 → Prp22.

The conclusions from immunoprecipitation studies rely on the assumption that epitopes are accessible to antibodies in the context of the splicing complex. Because the spliceosome is dynamic, we cannot rule out the formal possibility that accessibility of epitopes changes. However, the use of polyclonal antibodies diminishes this possibility.

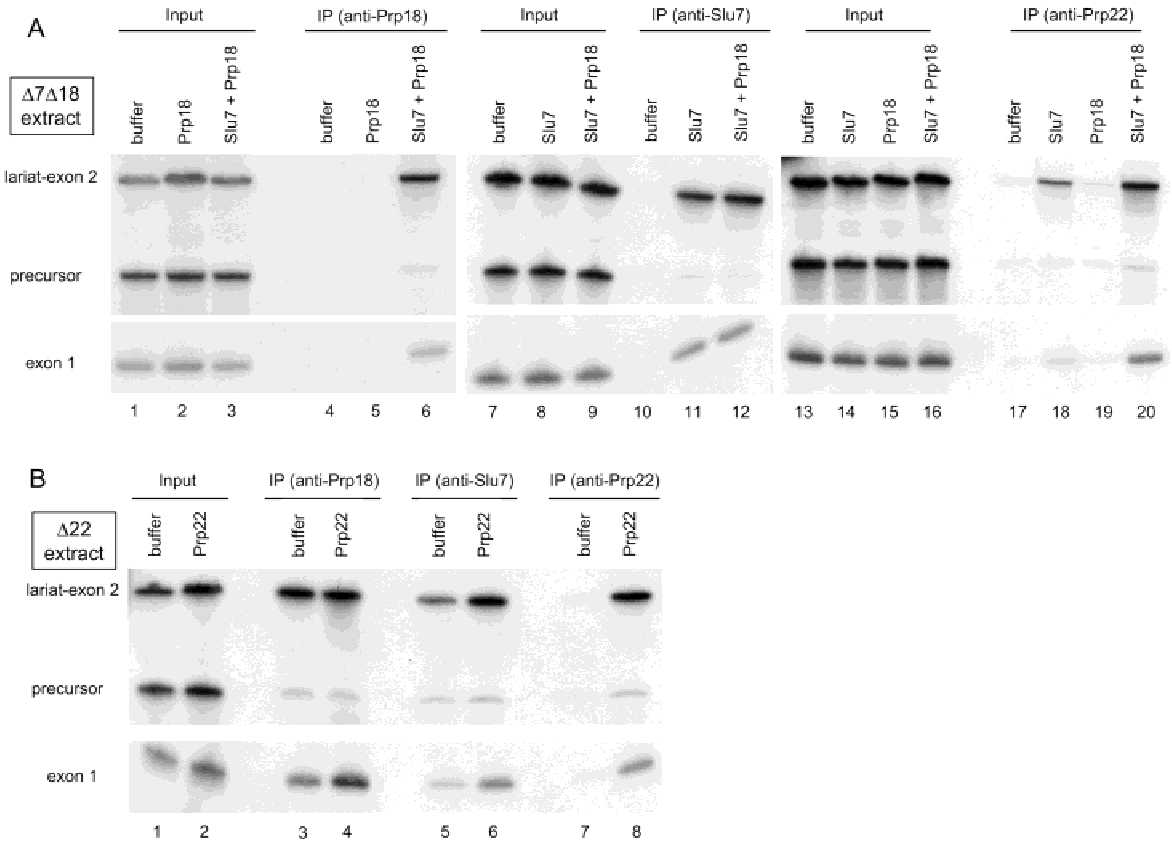

FIGURE 6. Interdependence of Slu7, Prp18, and Prp22 for spliceosome association. **A:** Splicing complexes containing lariat-exon 2 and exon 1 were formed on C303/305 precursor RNA in Δ7Δ18 extract. Aliquots were then supplemented with Prp18, Slu7, and Slu7 + Prp18 and subjected to immunoprecipitation with anti-Prp18, anti-Slu7, and anti-Prp22 antibodies. **B:** Splicing complexes containing lariat-exon 2 and exon 1 were formed on C303/305 precursor RNA in Δ22 extract. The reaction was supplemented with either buffer or with Prp22 protein and aliquots were subjected to immunoprecipitation with anti-Prp18, anti-Slu7, and anti-Prp22 antibodies.

Slu7, Prp18, and Prp22 leave the spliceosome prior to lariat-intron release

Previous studies showed that Slu7 and Prp22 remain bound to splicing complexes after the second transesterification step, insofar as mature mRNA could be precipitated when spliceosome disassembly was blocked by removal of ATP or by an ATPase-defective Prp22 mutant that did not catalyze mRNA release (Brys & Schwer, 1996; Schwer & Gross, 1998). After mRNA is released, Prp43 catalyzes the ATP-dependent release of excised lariat-introns (Martin et al., 2002). We employed dominant-negative mutants Prp22-Q804A and Prp43-T123A to block spliceosome disassembly prior to release of mature mRNA and of excised lariat-intron, respectively (Martin et al., 2002; Schneider et al., 2002). ^{32}P-labeled actin pre-mRNA was incubated in extracts that were supplemented with Prp22-Q804A or with Prp43-T123A (Fig. 7). The second transesterification step occurred and mRNA and lariat-intron formed (Fig. 7, lanes 1 and 7). Aliquots of the reaction mixtures were subjected to immunoprecipitation with antibodies against Prp16, Slu7, Prp18, Prp22, and Prp43. As expected, Prp16 was not associated with the spliceosomes after the second transesterification step (Fig. 7, lanes 2 and 8). When mRNA release was blocked by dominant-negative Prp22, anti-Prp18, anti-Slu7, and anti-Prp22 serum precipitated the products of steps 1 and 2, but not unspliced pre-mRNA (Fig. 7, lanes 3–5). In contrast, anti-Prp43 did not precipitate any ^{32}P-labeled RNA (Fig. 7, lane 6). When spliceosome disassembly was blocked at the Prp43-dependent step, antibodies against Slu7, Prp18, and Prp22 did not precipitate ^{32}P-labeled RNA. The remaining splicing complex, which contained excised lariat-intron, was precipitated with anti-Prp43 antibodies only (Fig. 7, lane 12). Thus, Slu7, Prp18, and Prp22 dissociate from the spliceosome prior to the Prp43-catalyzed release of lariat-intron.

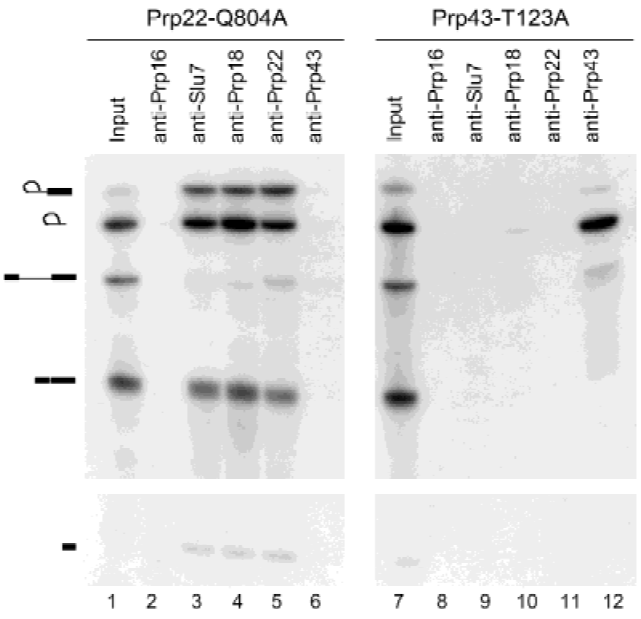

FIGURE 7. ^{32}P-labeled actin pre-mRNA was reacted with yeast whole-cell extract in the presence of either Prp22-Q804A or Prp43-T123A proteins for 25 min at 23 °C. Aliquots (10 μL) were withdrawn and served as input. Aliquots (30 μL) of the remaining sample were immunoprecipitated with anti-Prp16, anti-Slu7, anti-Prp18, anti-Prp22, and anti-Prp43 antibodies. RNAs were analyzed by denaturing PAGE and autoradiography. The symbols at the left indicate (from top to bottom) lariat-exon 2, lariat-intron, precursor, mRNA, and exon 1.

DISCUSSION

Trans-acting factors required specifically for the second transesterification step of splicing include Prp16, Slu7, Prp18, and Prp22. The second step can be divided into two stages, an ATP-dependent stage catalyzed by the DEAH-box ATPase Prp16, and an ATP-independent stage during which Slu7, Prp18, and Prp22 act. This study illuminates the mechanism of step 2 by showing that: (1) Slu7, Prp18, and Prp22 associate with the spliceosome in an ordered and interdependent fashion, (2) Slu7 contains two functionally important regions, and (3) the physical interaction between Slu7 and Prp18 is important for their cooperation in splicing.

The zinc knuckle motif has been implicated in RNA binding based on mutational and structural studies of retroviral nucleocapsid proteins, where the cysteine-rich region is crucial for packaging the viral genome (Dannull et al., 1994; Amarasinghe et al., 2000). Zinc knuckle motifs are also found in the splicing factors SF1/BBP and 9G8. In addition, the branchpoint binding protein SF1/BBP and the SR protein 9G8 also contain well-characterized RNA binding domains (Cavaloc et al., 1994; Arning et al., 1996). In SF1, the hnRNP K homology domain, but not the zinc knuckle, is crucial for binding of the protein to the branchpoint RNA and for assembly of the prespliceosomal complex in vitro (Rain et al., 1998; Liu et al., 2001). The SR protein 9G8 binds to RNA via its RNA binding domain and mutations in the zinc knuckle do not abolish RNA binding. However, zinc knuckle mutations alter the RNA binding specificity of 9G8 (Cavaloc et al., 1999). The importance of the zinc knuckle for Slu7 function has been unclear, as deletion of the domain or mutations at conserved positions within this region are inconsequential for cell growth (Frank & Guthrie, 1992; Zhang & Schwer, 1997). We now show that the zinc knuckle is involved in binding of Slu7 to the spliceosome and that it is crucial for Slu7 function in vitro in the absence of Prp18 or when the physical interaction with Prp18 is disrupted. This provides a plausible explanation for the observed lethality of Slu7 mutants in which both the zinc knuckle region and the Prp18 interaction are disrupted (Fig. 2), thus showing that either one of these two domains is necessary for Slu7 function.

Our data suggest a model in which Slu7, Prp18, Prp22, and Prp43 associate with the spliceosome in an or-

dered and interdependent fashion (Fig. 8). Slu7 can bind to the spliceosome in the absence of Prp18 and the zinc knuckle region is important for this binding. The simplest interpretation is that Slu7 contacts the spliceosome through its zinc knuckle. However, because the zinc knuckle is not essential, other mechanisms must exist for Slu7 to enter the spliceosome, and the alternative pathway is facilitated by Prp18. It remains to be determined whether Slu7 contacts protein or RNA components of the spliceosome. Thus far, we have been unable to detect discrete Slu7-RNA complexes in a gel-shift assay. In any event, the initial binding of Slu7 leads to the recruitment of Prp18 and to stabilization of the Slu7 interaction with the spliceosome. To exert this effect, Prp18 must physically interact with Slu7 on the spliceosome.

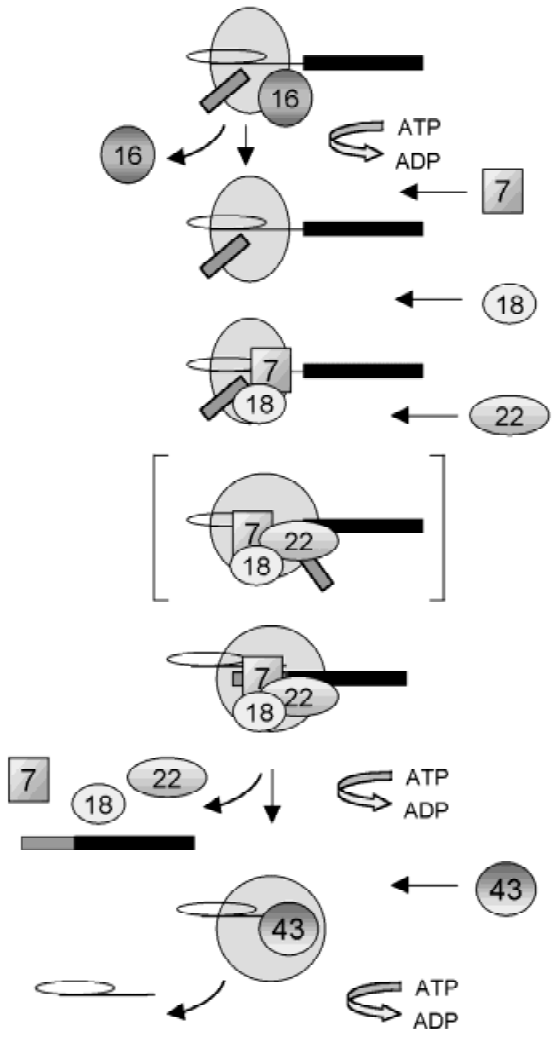

FIGURE 8. Model depicting the ordered recruitment of splicing factors Prp16 (16), Slu7 (7), Prp18 (18), Prp22 (22), and Prp43 (43) to the splicing complex containing lariat-exon 2 and exon 1. The spliceosome is shown as a shaded sphere, exon 1 and exon 2 as gray and black rectangles, respectively, and the intron is drawn as a line. The steps at which ATP is hydrolyzed are indicated. The bracketed spliceosomal complex can be detected only when the second transesterification step is blocked by a mutation in the 3′ splice site (in the C303/305 precursor RNA). The positions of the highlighted protein factors within the spliceosome are not intended to indicate specific binding to the RNA.

The findings that yeast whole-cell extract can be specifically depleted of Slu7 and Prp18 and addition of individual recombinant proteins can overcome the splicing defects is consistent with a recruitment model and argues against the idea that Slu7 and Prp18 proteins are tightly associated in yeast extract. Candidate targets within the spliceosome for binding to Slu7 and Prp18 are the U5 snRNP and the DExH-box protein Brr2. This is suggested by genetic interactions, such as the pair-wise synthetic lethality between conditional U5 snRNA, *slu7* and *prp18* mutants, by an observed two-hybrid interaction between Slu7 and Brr2, by coprecipitation of U5 snRNA with Prp18 antibodies, and by the functional involvement of the U5 snRNP in the selection and recognition of the 3′ splice site—the stage at which Slu7 and Prp18 act (Frank et al., 1992; Horowitz & Abelson, 1993a; Jones et al., 1995; Umen & Guthrie, 1995b; van Nues & Beggs, 2001).

Once Slu7 and Prp18 are bound to the spliceosome, Prp22 is recruited. A reported two-hybrid interaction between Prp22 and Slu7 (van Nues & Beggs, 2001) raises the possibility that Prp22 may be recruited through interaction with Slu7. With Slu7, Prp18, and Prp22 in place, the second transesterification reaction occurs, after which Prp22 catalyzes the ATP-dependent release of mRNA from the spliceosome (Schwer & Gross, 1998; Wagner et al., 1998). Concomitant with mRNA release, Slu7, Prp18, and Prp22 dissociate from the residual splicing complex containing the excised lariat-intron. At this stage, the RNA-dependent ATPase Prp43 binds to the remaining complex and catalyzes release of the lariat-intron (Martin et al., 2002).

MATERIALS AND METHODS

Site-directed mutagenesis of SLU7

Missense mutations were introduced into the *SLU7* gene using the two-stage PCR overlap extension method. Plasmid p358-SLU7(B) (*TRP1 CEN*) was used as a template for the first amplification step (Zhang & Schwer, 1997). The mutated DNA products of the second stage amplification were digested with *Nde*I and *Bam*HI restriction endonucleases and inserted into p358-SLU7(B) in lieu of the wild-type restriction fragment. The entire DNA segment was sequenced in order to confirm the presence of the desired mutation and to exclude the acquisition of unwanted mutations during amplification or cloning.

Test of mutational effects on SLU7 function in vivo by plasmid shuffle

Viability of the *slu7*Δ strain YXP3 (Mata *leu2 his7 trp1 slu7::hisG*) depends on p360-SLU7 (*URA3 CEN*), which complements the chromosomal deletion of *SLU7* (Zhang & Schwer,

1997). YXP3 was transformed with *TRP1 CEN* plasmids carrying the various *SLU7-Ala* mutants. Trp^+ transformants were selected and streaked to agar medium containing 0.75 mg/mL 5-FOA to select against maintenance of the *URA3* gene on p360-SLU7. The mutants' ability to support growth on 5-FOA was tested at 25 °C and 30 °C. The 5-FOA survivors were streaked onto YPD medium and incubated at different temperatures ranging from 15 °C to 37 °C.

Preparation of depleted splicing extracts

Yeast whole-cell extract from BJ2168 cells was prepared by grinding in liquid nitrogen as described (Ansari & Schwer, 1995). Antibodies against Slu7, Prp18, and Prp22 were affinity-purified using GST-Slu7, GST-Prp18, and GST-Prp22(1-480) polypeptides, purified from bacteria and coupled to Affigel-10 resin (BioRad) according to the vendor's protocol. Because the antisera had been raised against the His-tagged proteins, and because our complementation experiments were carried out with His-tagged recombinant proteins, this ensured that the antibody preparations were specific and did not contain antibodies against the His epitope. Aliquots of 120-μL extract were incubated with 15 μL of affinity-purified Slu7 antibodies (2.5 mg/mL in PBS) and 45 μL anti-Prp18 antibody (1.1 mg/mL in PBS) on ice for 45 min. Protein A Sepharose (150 μL of a 10-mg/mL slurry) was prewashed with PBS and then mixed with the extract/antibody mixture for 45 min. The resin was collected by centrifugation and the supernatant (Δ7Δ18 extract) was used for in vitro splicing assays.

Pre-mRNA splicing in vitro

^{32}P-labeled actin precursor RNA (or the mutant version C303/305) was synthesized by T7 RNA polymerase and purified by gel filtration through Sepharose CL-6B. Splicing reactions mixtures (10 μL) containing 60% extract (Δ7Δ18), 60 mM potassium phosphate, pH 7.0, 2.5 mM $MgCl_2$, 2 mM ATP, 3% (w/v) PEG_{8000}, and ~2 fmol pre-mRNA were incubated at 23 °C for 15 min to allow for step 1 to occur. Then, 30 ng of protein were added to chase the products of step 1 to mature mRNA. The reaction products were analyzed by electrophoresis through a 6% polyacrylamide gel containing 7 M urea in TBE. The labeled RNA was visualized by autoradiography and quantified using a phosphorimager.

Expression of Slu7 and Prp18 in bacteria

DNA fragments encoding the various Slu7 mutants were digested with *Nde*I and *Bam*H1 and inserted into expression vectors pET16b and pET3c. The DNA fragment carrying PRP18 was inserted into pET14b. In pET16b and pET14b, the ORFs are fused to an N-terminal His_{10} or His_6 peptide, respectively. The resulting plasmids were transformed into the *E. coli* strain BL21(DE3). Cultures were inoculated from single colonies of freshly transformed cells and maintained in logarithmic growth at 37 °C in LB medium containing 0.1 mg/mL ampicillin to a final volume of 0.5 L. When the A_{600} reached 0.6 to 0.8, the cultures were chilled on ice for 30 min, adjusted to 0.4 mM isopropyl β-*D*-thiogalactopyranoside (IPTG) and incubated for 16 h at 17 °C with constant shaking. Cells were harvested by centrifugation and the pellets were stored at −80 °C.

Purification of His-Slu7 and His-Prp18

All procedures were performed at 4 °C. The cell pellet was resuspended in 50 mL buffer A (50 mM Tris-HCl, pH 7.5, 250 mM NaCl, 10% sucrose, and lysozyme at 0.2 mg/mL final concentration). The suspension was incubated for 45 min, then adjusted to 0.1% Triton X-100 and incubated for an additional 15 min. The lysate was sonicated to reduce viscosity and centrifuged for 30 min at 13,000 rpm in a Sorvall SS34 rotor to remove insoluble material. The soluble fraction was mixed with 3.5 mL (50% slurry) of nickel-NTA agarose beads (Qiagen) for 1 h. The resin was collected by centrifugation and then subjected to repeated cycles of washing with buffer A and centrifugation. The mixture was poured into a column and the absorbed proteins eluted stepwise with 5-mL aliquots of 25, 100, and 500 mM imidazole in Buffer B (50 mM Tris-HCl, pH 7.5, 250 mM NaCl, and 10% glycerol). Fractions of 1.5 mL were collected and the elution profile was monitored by SDS-PAGE. Peak fractions containing the Slu7 and Prp18 polypeptides (100 mM imidazole eluate) were pooled and dialyzed against Buffer E (50 mM Tris-HCl, pH 7.5, 50 mM NaCl, 15% glycerol). Protein concentrations were determined using Bradford dye reagent (BioRad), with bovine serum albumin as a standard.

Untagged Slu7 polypeptides were produced in bacteria by cloning the SLU7 genes into pET3c and inducing recombinant protein expression by IPTG induction as described above. The Slu7 proteins were removed from soluble bacterial lysates by precipitation with 40% ammonium sulfate. The precipitates were resuspended in buffer B and then dialyzed against buffer B.

Immunoprecipitation of splicing complexes

Aliquots (5 μL) of affinity-purified antibodies were bound to 40 μL Protein A sepharose in 400 μL of IPP_{500} (10 mM Tris-HCl, pH 8.0, 500 mM NaCl, 0.1% NP-40). Splicing reactions were carried out in 40-μL aliquots, supplemented with Prp18 and Slu7 proteins or the buffer control. Aliquots of each reaction mixture (10 μL) were extracted and served as input, and the remainder (30 μL) was incubated with the bead-bound antibodies in 200 μL IPP_{150} (10 mM Tris-HCl, pH 8.0, 150 mM NaCl, 0.1% NP-40) for 1 h at 4 °C with constant mixing. The beads were then collected by centrifugation and washed with IPP_{150} (3 × 200 μL). The RNA products in the bead pellet were extracted, analyzed by denaturing PAGE, and visualized by autoradiography. The amount of RNA in the input and the immunoprecipitated fractions were quantified using a phosphorimager. The efficiency of immunoprecipitation was 20–30% of input for splicing intermediates and ~1% for precursor RNA.

To arrest spliceosomes at the Prp22-dependent stage (release of mRNA) and at the Prp43-dependent stage (release of lariat-intron), splicing reaction mixtures (170 μL) containing whole-cell extract and 1.3 μg Prp22-Q804A or 0.9 μg Prp43-T123A were incubated at 23 °C for 25 min. An aliquot (10 μL) of each reaction served as input and 30 μL were used for immunoprecipitation with the various antibodies in IPP_{150} as described above.

Slu7-Prp18 interaction in vitro

Purified His_6-Prp18 (64 μg) was mixed with partially purified Slu7 proteins (180 μg) in buffer I (50 mM Tris-HCl, pH 7.4, 250 mM NaCl, 20 mM imidazole) in a final volume of 400 μL. The mixtures were added to 50 μL Ni-NTA resin (50% slurry) equilibrated in buffer I and gently mixed for 60 min at 4 °C. The resin was collected by centrifugation and the supernatants reserved. The pellets were washed extensively with buffer I. Bound proteins were eluted with 150 μL of 50 mM Tris-HCl (pH 7.4), 250 mM Nacl, 500 mM imidazole. An equal volume of 2× SDS-loading buffer was added and the samples were analyzed by electrophoresis through a 10% polyacrylamide gel containing 0.01% SDS and stained with Coomassie dye.

ACKNOWLEDGMENTS

We thank David Horowitz and Susanne Schneider for stimulating discussions and comments on the manuscript. This work was supported by National Institutes of Health Grant GM50288.

Received May 16, 2002; returned for revision June 3, 2002; revised manuscript received June 10, 2002

REFERENCES

Amarasinghe GK, De Guzman RN, Turner RB, Chancellor KJ, Wu ZR, Summers MF. 2000. NMR structure of the HIV-1 nucleocapsid protein bound to stem-loop SL2 of the psi-RNA packaging signal. Implications for genome recognition. *J Mol Biol 301*: 491–511.

Ansari A, Schwer B. 1995. SLU7 and a novel activity, SSF1, act during the PRP16-dependent step of yeast pre-mRNA splicing. *EMBO J 14*:4001–4009.

Arning S, Grüter P, Bilbe G, Krämer A. 1996. Mammalian splicing factor SF1 is encoded by variant cDNAs and binds to RNA. *RNA 2*:794–810.

Ben-Yehuda S, Dix I, Russell CS, McGarvey M, Beggs JD, Kupiec M. 2000. Genetic and physical interactions between factors involved in both cell cycle progression and pre-mRNA splicing in *Saccharomyces cerevisiae*. *Genetics 156*:1503–1517.

Brys A, Schwer B. 1996. Requirement for SLU7 in yeast pre-mRNA splicing is dictated by the distance between the branchpoint and the 3′ splice site. *RNA 2*:707–717.

Burge CB, Tuschl T, Sharp PA. 1999. Splicing of precursors to mRNA by the spliceosome. In Gesteland RF, Atkins JF, eds. *The RNA world*, 2nd ed. Cold Spring Harbor, New York: Cold Spring Harbor Laboratory Press. pp 525–560.

Cavaloc Y, Bourgeois CF, Kister L, Stevenin J. 1999. The splicing factors 9G8 and SRp20 transactivate splicing through different and specific enhancers. *RNA 5*:468–483.

Cavaloc Y, Popielarz M, Fuchs JP, Gattoni R, Stevenin J. 1994. Characterization and cloning of the human splicing factor 9G8: A novel 35 kDa factor of the serine/arginine protein family. *EMBO J 13*:2639–2649.

Chua K, Reed R. 1999. Human step II splicing factor hSlu7 functions in restructuring the spliceosome between the catalytic steps of splicing. *Genes & Dev 13*:841–850.

Dannull J, Surovoy A, Jung G, Moelling K. 1994. Specific binding of HIV-1 nucleocapsid protein to PSI RNA in vitro requires N-terminal zinc finger and flanking basic amino acid residues. *EMBO J 13*:1525–1533.

Frank D, Guthrie C. 1992. An essential splicing factor, SLU7, mediates 3′ splice site choice in yeast. *Genes & Dev 6*:2112–2124.

Frank D, Patterson B, Guthrie C. 1992. Synthetic lethal mutations suggest interactions between U5 small nuclear RNA and four proteins required for the second step of splicing. *Mol Cell Biol 12*:5197–5205.

Horowitz DS, Abelson J. 1993a. A U5 small nuclear ribonucleoprotein particle protein involved only in the second step of pre-mRNA splicing in *Saccharomyces cerevisiae*. *Mol Cell Biol 13*:2959–2970.

Horowitz DS, Abelson J. 1993b. Stages in the second reaction of pre-mRNA splicing: The final step is ATP independent. *Genes & Dev 7*:320–329.

Jones MH, Frank DN, Guthrie C. 1995. Characterization and functional ordering of Slu7p and Prp17p during the second step of pre-mRNA splicing in yeast. *Proc Natl Acad Sci USA 92*: 9687–9691.

Käufer NF, Potashkin J. 2000. Analysis of the splicing machinery in fission yeast: A comparison with budding yeast and mammals. *Nucleic Acids Res 28*:3003–3010.

Liu Z, Luyten I, Bottomley MJ, Messias AC, Houngninou-Molango S, Sprangers R, Zanier K, Krämer A, Sattler M. 2001. Structural basis for recognition of the intron branch site RNA by splicing factor 1. *Science 294*:1098–1102.

Madhani HD, Guthrie C. 1994. Dynamic RNA–RNA interactions in the spliceosome. *Annu Rev Genet 28*:1–26.

Martin A, Schneider S, Schwer B. 2002. Prp43 is an essential RNA-dependent ATPase required for release of lariat-intron from the spliceosome. *J Biol Chem 277*:17743–17750.

Moore MJ, Query CC, Sharp PA. 1993. Splicing of precursors to mRNA by the spliceosome. In Gesteland RF, Atkins JF, eds. *Splicing of precursors to mRNA by the spliceosome*. Cold Spring Harbor, New York: Cold Spring Harbor Laboratory Press. pp 303–357.

Newman AJ. 1997. The role of U5 snRNP in pre-mRNA splicing. *EMBO J 16*:5797–5800.

Nilsen TW. 1994. RNA–RNA interactions in the spliceosome: Unraveling the ties that bind. *Cell 78*:1–4.

Rain JC, Rafi Z, Rhani Z, Legrain P, Krämer A. 1998. Conservation of functional domains involved in RNA binding and protein–protein interactions in human and *Saccharomyces cerevisiae* pre-mRNA splicing factor SF1. *RNA 4*:551–565.

Rymond BC, Rosbash M. 1985. Cleavage of 5′ splice site and lariat formation are independent of 3′ splice site in yeast mRNA splicing. *Nature 317*:735–737.

Schneider S, Hotz HR, Schwer B. 2002. Characterization of dominant-negative mutants of the DEAH-box splicing factors Prp22 and Prp16. *J Biol Chem 277*:15452–15458.

Schwer B, Guthrie C. 1991. PRP16 is an RNA-dependent ATPase that interacts transiently with the spliceosome. *Nature 349*: 494–499.

Schwer B, Guthrie C. 1992. A conformational rearrangement in the spliceosome is dependent on PRP16 and ATP hydrolysis. *EMBO J 11*:5033–5039.

Schwer B, Gross CH. 1998. Prp22, a DExH-box RNA helicase, plays two distinct roles in yeast pre-mRNA splicing. *EMBO J 17*: 2086–2094.

Staley JP, Guthrie C. 1998. Mechanical devices of the spliceosome: Motors, clocks, springs, and things. *Cell 92*:315–326.

Stevens SW, Ryan DE, Ge HY, Moore RE, Young MK, Lee TD, Abelson J. 2002. Composition and functional characterization of the yeast spliceosomal penta-snRNP. *Mol Cell 9*:31–44.

Umen JG, Guthrie C. 1995a. A novel role for a U5 snRNP protein in 3′ splice site selection. *Genes & Dev 9*:855–868.

Umen JG, Guthrie C. 1995b. The second catalytic step of pre-mRNA splicing. *RNA 1*:869–885.

van Nues RW, Beggs JD. 2001. Functional contacts with a range of splicing proteins suggest a central role for Brr2p in the dynamic control of the order of events in spliceosomes of *Saccharomyces cerevisiae*. *Genetics 157*:1451–1467.

Vijayraghavan U, Parker R, Tamm J, Iimura Y, Rossi J, Abelson J, Guthrie C. 1986. Mutations in conserved intron sequences affect multiple steps in the yeast splicing pathway, particularly assembly of the spliceosome. *EMBO J 5*:1683–1695.

Wagner JDO, Jankowsky E, Company M, Pyle AM, Abelson JN. 1998. The DEAH-box protein PRP22 is an ATPase that mediates ATP-dependent mRNA release from spliceosomes and unwinds RNA duplexes. *EMBO J 17*:2926–2937.

Zhang X, Schwer B. 1997. Functional and physical interaction between the yeast splicing factors Slu7 and Prp18. *Nucleic Acids Res 25*:2146–2152.